Materials Science & Engineering C 93 (2018) 170–177

Contents lists available at ScienceDirect

Materials Science & Engineering C

journal homepage: www.elsevier.com/locate/msec

Collagen-silica nanocomposites as dermal dressings preventing infection *in vivo*

Andrea M. Mebert[a], Gisela S. Alvarez[a], Roxana Peroni[b], Corinne Illoul[c], Christophe Hélary[c], Thibaud Coradin[c], Martin F. Desimone[a,*]

[a] Universidad de Buenos Aires, Consejo Nacional de Investigaciones Científicas y Técnicas (CONICET), Instituto de la Química y Metabolismo del Fármaco (IQUIMEFA), Facultad de Farmacia y Bioquímica, Buenos Aires, Argentina
[b] Pharmacology Research Institute, University of Buenos Aires and National Science Research Council (CONICET), Department of Pharmacology, Facultad de Farmacia y Bioquímica, Buenos Aires, Argentina
[c] Sorbonne Université, CNRS, Collège de France, Laboratoire de Chimie de la Matière Condensée de Paris, 4 place Jussieu, F-75005 Paris, France

ARTICLE INFO

Keywords:
Collagen
Silica
Nanocomposite
Antibacterial
Gentamicin
Rifamycin
Dual delivery

ABSTRACT

The controlled delivery of multiple drugs from biomaterials is a timely challenge. In particular the nanocomposite approach offers a unique opportunity to combine the scaffold-forming ability and biocompatibility of hydrogels with the versatile and tunable drug release properties of micro- or nano-carriers. Here, we show that collagen-silica nanocomposites allowing for the prolonged release of two topical antibiotics are promising medicated dressings to prevent infection in wounds. For this purpose, core–shell silica particles loaded with gentamicin sulfate and sodium rifamycin were combined with concentrated collagen type I hydrogels. A dense fibrillar network of collagen exhibiting its typical periodic banding pattern and a homogenous particle distribution were observed by scanning electron microscopy. Antibiotics release from nanocomposites allowed a sustained antibacterial effect against *Staphylococcus aureus* over 10 days *in vitro*. The acute dermal irritation test performed on albino rabbit skin showed no sign of severe inflammation. The antibacterial efficiency of nanocomposites was evaluated *in vivo* in a model of cutaneous infection, showing a 2 log steps decrease in bacterial population when loaded systems were used. In parallel, the histological examination indicated the absence of M1 inflammatory macrophages in the wound bed after treatment. Taken together, these results illustrate the potentialities of the nanocomposite approach to develop collagen-based biomaterials with controlled dual drug delivery to prevent infection and promote cutaneous wound repair.

1. Introduction

Wound healing is a complex process that requires coordination between many types of cells and the extracellular microenvironment. In the case of impaired wound healing, wounds do not go through the regular sequences and are locked in a state of chronic inflammation. Such chronic wounds represent an immense financial burden on medical systems worldwide. In these situations, the control of infection is extremely important as it can ultimately lead to gangrene and even amputation. Therefore biomaterial-based wound therapy has been growing steadily [1,2], with an increasing interest for medicated wound dressings allowing for the delivery of antibiotics [3,4]. Type I collagen hydrogels are of particular interest in regenerative medicine. They are well-tolerated immunologically when implanted in the body. In addition, collagen gels are remodeled within living tissues, enhancing their potential for biointegration [5]. However, similarly to many others biopolymer hydrogels, collagen gels are usually poor drug delivery systems, due to their large porosity and strong hydrophilic character [6]. Composite approaches where drug-loaded particles are embedded in a scaffold have been shown to allow prolonged antibiotics, with release up to 4 weeks [7]. In this context, it was previously demonstrated that encapsulation of non-porous silica nanoparticles loaded with gentamicin within a collagen gel extended the antibiotic release time over one week *in vitro* [8].

The emergence of antibacterial resistance is a worldwide challenge. Infections by *S. aureus* remain as a frequent cause of morbidity and mortality, this bacterium showing extremely high capability to develop resistance against antibiotics, both by mutation and by DNA transfer. Most approaches are based on alternative therapies, such as photodynamic inhibition [9] or therapeutic antibodies [10], or using drug

* Corresponding author at: Junin 956, Ciudad Autónoma de Buenos Aires, Buenos Aires 1113, Argentina.
E-mail address: desimone@ffyb.uba.ar (M.F. Desimone).

https://doi.org/10.1016/j.msec.2018.07.078
Received 8 November 2017; Received in revised form 17 July 2018; Accepted 27 July 2018
Available online 29 July 2018
0928-4931/

delivery systems to co-administrate or improve "old" drugs, rather than developing new drugs that is expensive and time-consuming [11–13]. In this context, we have previously described the synthesis of modified core-shell silica nanoparticles loaded with two antibiotics, gentamicin in the core and rifamycin in the shell allowing for a dual therapeutic activity *in vitro* against *S. aureus* and *Pseudomonas aeruginosa*. It was shown that both antibiotics were effective in inhibiting *S. aureus* growth but their release from the silica nanocarriers was complete within 20 h [14].

Even though the preparation of nanocomposites based on natural polymers such as collagen containing antibiotic-loaded nanoparticles has been well described in the last years, the *in vivo* performance of these materials intended for use in wound healing as well as their biocompatibility and possible inflammatory reactions are still under investigation. For instance, bacterial cellulose gels with silver nanoparticles were assayed *in vivo* in rat models with second degree skin wounds and found to decrease bacterial population by a factor of 4 after four days and to achieve a higher rate of epithelialization [15]. In this context, we have developed here collagen-silica nanocomposites capable of delivering the two antibiotics with different mechanisms of action and bacterial spectra and demonstrate their skin innocuity and *in vivo* antibacterial efficiency.

2. Experimental

2.1. Materials

Tetraethyl orthosilicate (TEOS, 98%) and (3-mercaptopropyl) trimethoxysilane (MPTMOS, 95%) were purchased from Sigma-Aldrich, as well as the sodium rifamycin and gentamicin sulfate antibiotics. Ammonium hydroxide (30%) was obtained from Carlo Erba Reagents. All other reagents were of analytical grade and commercially available.

2.2. Gentamicin-loaded core silica particles synthesis

Bare silica nanoparticles (NP) measuring 300 nm in diameter were synthesized according to the Stöber method. Briefly, tetraethyl orthosilicate and ammonium hydroxide were added dropwise to a stirred solution of ultrapure water and absolute ethanol in the right proportions to obtain the desired size [16]. The solution was stirred overnight at room temperature. Particles were washed once with absolute ethanol, twice with deionized water, recovered by centrifugation and dried under vacuum.

Thiol grafting was accomplished by resuspending 5.51 g of bare silica particles in a mixture of 548 mL of absolute ethanol and 12 mL of ammonium hydroxide, and then 1% (in total volume) of MPTMOS was added [17]. The mixture was stirred for 40 min at room temperature and then the solvent was evaporated at 80 °C until 1/3 of the original volume was reached. Particles were washed twice with absolute ethanol, once with deionized water and recovered by centrifugation, dried under vacuum and stored in a closed flask.

Later, 3.6 g of thiol-modified NPs were resuspended in 180 mL of hydrogen peroxide 35% and left for 48 h under stirring. Then the particles were washed three times with ethanol and dried under vacuum. The resulting powder was resuspended in 150 mL of sulfuric acid and stirred for 2 h. Then the solution was slowly diluted in deionized water in a cold bath. The particles were recovered and washed with ethanol and deionized water by centrifugation, vacuum dried and stored.

Gentamicin loading was carried out by mixing the sulfonate-modified particles and the antibiotic in a ratio of 375 mg of particles: 20 mg of antibiotic: 50 mL of deionized water. Suspensions were stirred overnight at room temperature. The resulting particles were recovered by centrifugation and washed three times with deionized water, dried under vacuum and stored in a closed flask.

2.3. Synthesis of the shell and rifamycin loading

The silica shell layer synthesis was carried out by resuspending the core particles previously loaded with gentamicin in an ethanol–water medium to which tetraethyl orthosilicate and ammonium hydroxide were added dropwise with continuous stirring, in a 60 mg NP: 60 mL EtOH: 0.36 mL deionized water: 1.2 mL TEOS: 0.6 mL ammonium hydroxide ratio. The solution was stirred overnight at room temperature. The synthesized core-shell nanoparticles were washed once with absolute ethanol, twice with deionized water and then recovered by centrifugation and dried under vacuum.

Thiol modification was carried out by resuspending the particles in a mixture of absolute ethanol and ammonium hydroxide, and then adding MPTMOS to the mixture which was stirred for 40 min at room temperature, as previously described. Subsequently, the solvent was evaporated at 80 °C until 1/3 of the original volume was reached.

Finally, rifamycin was loaded by mixing the core-shell particles preloaded with gentamicin with the second antibiotic in deionized water in a ratio of 375 mg of particles: 20 mg of antibiotic: 50 mL of deionized water. The particles were washed and stored as described before.

2.4. Silica core-shell particles and collagen type I composites synthesis

Collagen type I was purified from rat tails as previously described [18]. Composites were prepared by resuspending 0.5 M core-shell silica particles in a 5 $mg{\cdot}mL^{-1}$ collagen suspension in 0.5 M acetic acid. The suspension was then dispensed into 96-well plates (200 μL) and left exposed to ammonium vapors overnight at room temperature for collagen gelling. Later, the plates were ventilated and washed with PBS solution until neutral pH was reached.

2.5. Scanning electron microscopy (SEM) analysis

The core-shell nanocomposites were analyzed using a Zeiss Supra 40 microscope for Scanning Electron Microscopy (SEM). For this purpose, samples without cells were washed three times with PBS, fixed with a 2.5% glutaraldehyde in PBS solution for 1 h at 4 °C, freeze-dried and subjected to gold sputtering prior to analysis.

2.6. Fourier-transform infrared spectroscopy

FT-IR spectroscopy was performed using a Nicolet is 50 FT-IR spectrophotometer, with a KBr beamsplitter, and spectra were recorded with a resolution of 2 cm^{-1} using a DTGS detector. The samples were measured using the Attenuated total reflectance (ATR) technique.

2.7. Determination of minimum inhibitory concentrations

The minimum inhibitory concentrations (MICs) were determined in liquid medium. For this purpose, *Staphylococcus aureus* ATCC 289213 was used as the sensitive microorganism. The drugs or nanoparticles were added at five different concentrations to freshly-prepared 1×10^6 $CFU{\cdot}mL^{-1}$ bacterial suspensions in growth media. After overnight incubation at 37 °C, MICs were determined as the concentrations between the maximum concentrations where visible growth could be appreciated and the minimum concentrations where it could not. The concentrations tested were 0.01 to 10 $\mu g{\cdot}mL^{-1}$ for gentamicin sulfate, and 0.001 to 1 $\mu g{\cdot}mL^{-1}$ for sodium rifamycin. The inhibitory effect of the combination of both drugs was also tested. Nanoparticles were tested in a concentration range of 0.0017 to 1.7 $mg{\cdot}mL^{-1}$. Bacterial suspensions in growth media without added antibiotics or nanoparticles were used as controls.

2.8. Antibacterial activity

The microbiological assay was carried out using the disk diffusion

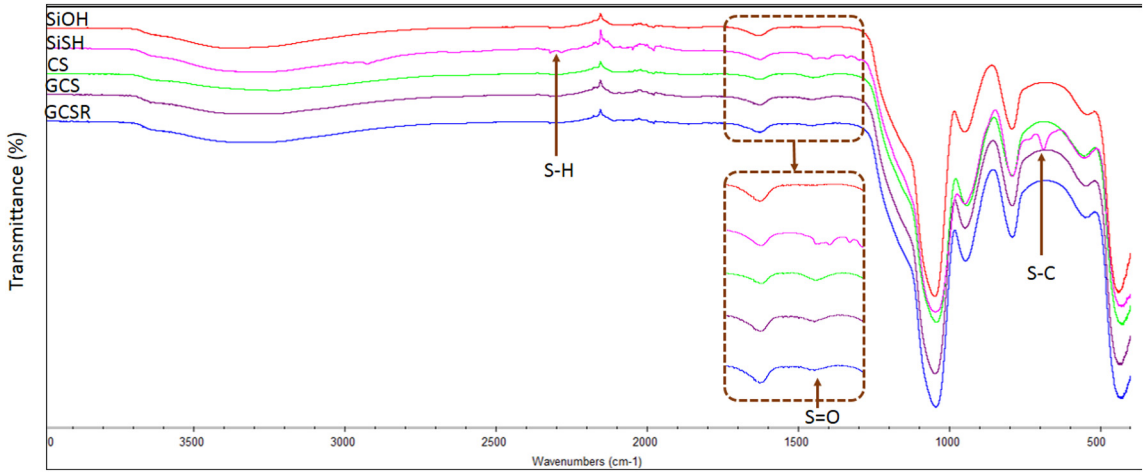

Fig. 1. FTIR spectra of Silica Nanoparticles (SiOH), thiolated (SiSH), unloaded (CS), single loaded with gentamicin (GCS) and double loaded core-shell nanoparticles (GCSR).

method as described in the US Pharmacopeia. *S. aureus* ATCC 289213 was used as the sensitive microorganism. Petri dishes with 2 to 5 mm thick Mueller-Hinton agar medium were used throughout this experiment as growth media. Briefly, 100 µL of a 1×10^7 CFU·mL^{-1} bacterial suspension in PBS was homogenously scattered through the agar surface. Subsequently, 200 µL of double drug-loaded composites and unloaded composites (control) were leaned and gently pushed on the inoculated agar surface. Gentamicin-loaded sterile absorbent paper disks of same dimension were used as reference and positive controls in concentrations ranging from 20 to 120 µg·mL^{-1}. The inhibition zone was measured after overnight incubation at 37 °C. Then the recovered composite was deposited on a new inoculated agar plate with fresh bacteria and gentamicin standards. This process was repeated 10 times.

2.9. Superficial skin infection

In vivo assays were carried out in male Wistar rats (280–350 g body weight). Animals were housed under a 12: 12 h light: dark cycle, at controlled room temperature with food and water *ad libitum*. All procedures involving animals were conducted in accordance with NIH guidelines for the Care and Use of Laboratory Animals (Institutional Animal Care and Use Committee Guidebook, 2nd ed., 2002). Animal treatment was carried out in accordance with the guidelines of the 6344/96 regulation of the Argentinean National Drug, Food and Medical Technology Administration (ANMAT).

The rats were anesthetized with a mixture of 40 mg·kg^{-1} ketamine hydrochloride and 10 mg·kg^{-1} xylazine hydrochloride i.p. The fur from the dorsal area of the trunk of the test animals was shaved carefully avoiding skin abrasion. Small areas (1 cm^2) were irritated scrapping with the aid of a scalpel until the skin became visibly damaged and was characterized by reddening and glistening but no regular bleeding occurred [19]. Staphylococcal infection was carried out by disposing 5 µL of and 1×10^8 bacterial suspension. Infected zones were covered with 200 µL double drug-loaded or unloaded nanocomposites (control) and protected with a band aid. After 48 h the animals were euthanized by inhalation of CO_2 in a chamber at a fill rate of 10–30% volume per minute displacement during 10 min. The tested skin zones were removed.

For bacterial recount, the skin was disaggregated in sterile PBS (5 mL), then serial dilutions in PBS were made to reach an appropriated number of colonies to count accurately after spreading on an agar plated. Plates were incubated overnight at 37 °C.

Histological examination was carried out by fixation of the treated skin with 3.5% formaldehyde for 24 h and preparation of paraffin blocks. Hematoxylin-Eosin, Masson Trichrome and Giemsa staining of the animal skin was performed and observed with a Carl Zeiss AxioVert A1 microscope.

2.10. Acute dermal irritation test

The assay was performed according to Test No. 404: Acute Dermal Irritation/Corrosion of the OECD Guidelines for the Testing of Chemicals [20].

Albino rabbits were used to test the nanocomposites. For this purpose, 0.5 g of the nanocomposites was applied to a small area of skin (approximately 6 cm^2) of an experimental animal; untreated skin areas of the test animal served as the control. The exposure period was 24 h. Residual nanocomposites were then removed and all animals were examined for signs of erythema and edema after 1, 24, 48 and 72 h.

2.11. Statistical analysis

In all cases data are mean ± SD of triplicate experiments. The differences were analyzed using two-way ANOVA, followed by the Tukey post-test; $P < 0.05$ was considered significant.

3. Results and discussion

Core-shell silica nanoparticles with a diameter of 336 ± 43 nm loaded with both gentamicin and rifamycin were prepared according to a previously-described protocol [14]. Core-shell nanoparticles were designed to allow the maximum antibiotic loading. As we described before, gentamicin, a positively charged molecule, interacts with strongly negative surfaces such as sulfonate-grafted silica nanoparticles. In the case of rifamycin, a higher loading capacity was found with thiol-modified particles, which could be attributed to non-covalent hydrophobic interactions. A more detailed characterization of these particles was previously carried out. Briefly, core nanoparticles exhibiting a surface-modified with sulfonate groups allowed for significant adsorption of gentamicin (5950 µg·g^{-1}) while a silica shell layer grafted with mercaptopropyl groups, allowed for adsorption of rifamycin (670 µg·g^{-1}) [14].

Through the analysis of IR spectra presented in Fig. 1, it was possible to follow the successive steps of particle preparation. First, the grafting of the thiol-bearing silanes could be evidenced by peaks at *ca.* 2300 cm^{-1} and 700 cm^{-1}, assigned to S—H and C—S vibrations that are present on the SiSH spectrum. The oxidation of thiol groups to sulfonates was confirmed by a characteristic peak at 1450 cm^{-1} due to the asymmetric stretch of the S═O group in CS particles, which decreases in intensity after addition of antibiotics. However, the previously

Table 1
Minimum inhibitory concentration (MIC) of rifamycin and gentamicin antibiotics (ATB) and unloaded core-shell nanoparticles (CS), gentamicin single-loaded (GCS) or gentamicin and rifamycin double-loaded (GCSR) core-shell nanoparticles. MIC NP: concentration of nanoparticles needed to observed an inhibitory effect.

Nanoparticle	Antibiotic	MIC $_{ATB}$ ($\mu g \cdot mL^{-1}$)	MIC $_{NP}$ ($mg \cdot mL^{-1}$)
	Gentamicin	3.03	
	Rifamycin	0.055	
CS			> 1.70
GCS		2.96	0.51
GCSR	Gentamicin	0.55	0.093
	Rifamycin	0.062	

discussed peaks at 2300 and 700 cm^{-1} were no longer visible after the synthesis of the thiolated shell probably due to the small thickness of this added silica layer. In fact, the size of $SiSO_3$ nanoparticles calculated by TEM does not significantly differ from that of CS particles [14].

The minimum inhibitory concentration (MIC), *i.e.* the lowest concentration that inhibits the visible growth of a microorganism after overnight incubation [21], of the different particles was determined against *S. aureus* (Table 1). While no antibacterial effect could be measured for the antibiotic-free core-shell particles (CS) up to a 1.7 $mg \cdot mL^{-1}$ concentration, the MIC of gentamicin-loaded core-shell particles (GCS) was found to be 0.51 $mg \cdot mL^{-1}$, whereas *ca.* 5 times less gentamicin/rifamycin double-loaded core-shell nanoparticles (GCSR)

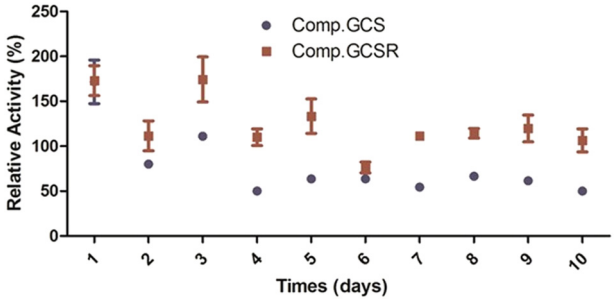

Fig. 3. Relative percentage of the inhibition zone generated by the nanocomposites in comparison to a 60 $\mu g \cdot mL^{-1}$ gentamicin standard after 10 days of consecutive experiments. Comp.Gcs: single-loaded nanocomposites carrying only gentamicin, Comp.GcsR: double loaded nanocomposites with gentamicin and rifamycin.

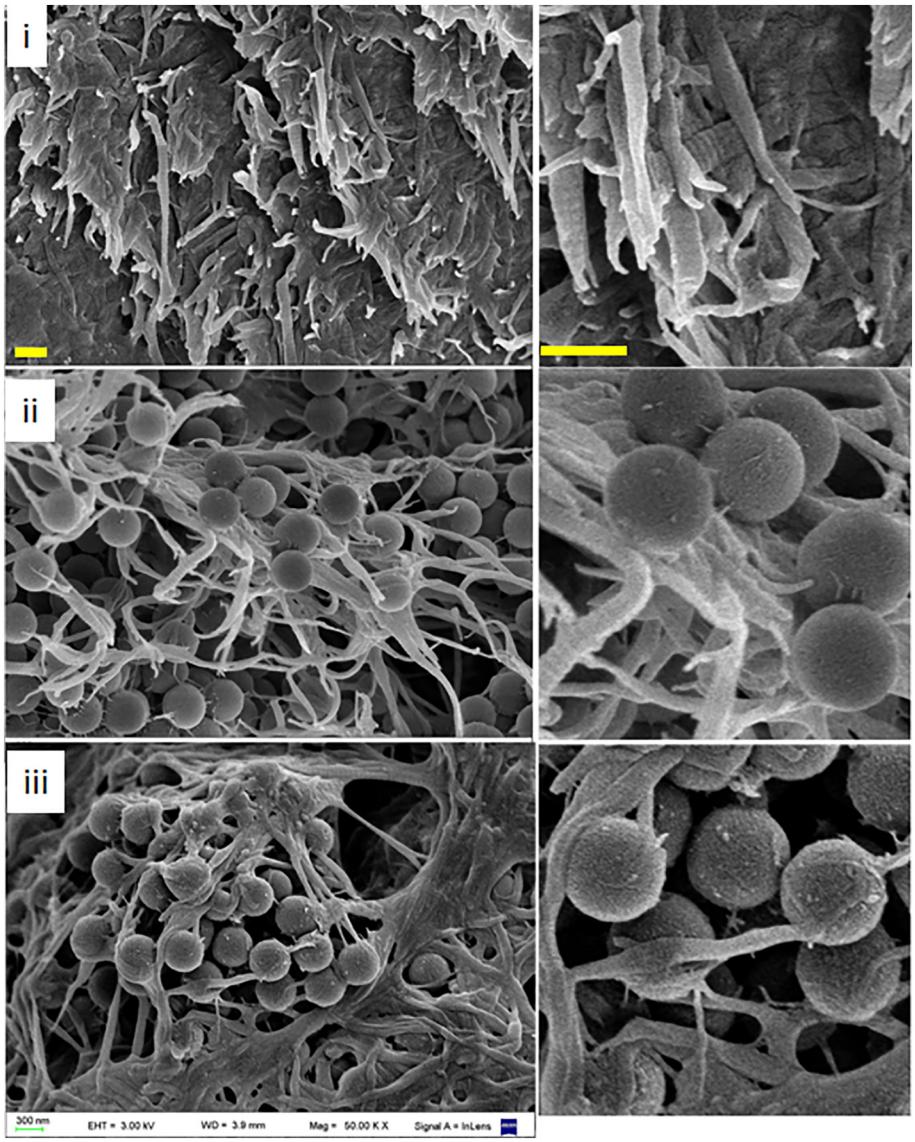

Fig. 2. *Left* SEM image (i) collagen hydrogel, (ii) unloaded and (iii) double loaded core-shell-collagen composite. *Right.* Close up view. Scale 300 nm.

(A)

(B)

DERMAL LESIONS IN RABBITS						
	Animal 1		Animal 2		Animal 3	
Time (h)	male		female		female	
	A	B	A	B	A	B
1	0	0	0	0	0	0
24	0	0	0	0	0	0
48	0	0	0	0	0	0
72	0	0	0	0	0	0
	0.00		0.00		0.00	

Fig. 4. (A) Albino rabbit skin 72 h after exposure to double loaded core-shell silica nanocomposites. (B) Dermal injuries observed among 72 h. A- Erythema B- Edema. Scale 0: not observed; 1: slightly; 2: well define; 3: moderate; 4: severe.

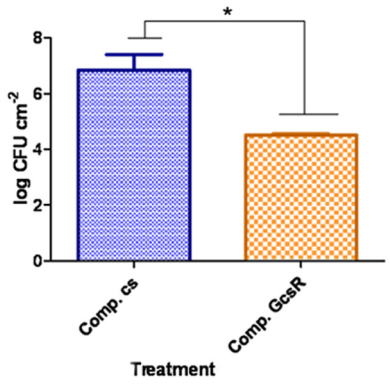

Fig. 5. Number of bacteria per cm^2 of skin of animals tested. Blue: core-shell nanocomposites with unloaded nanoparticles (comp.cs) Orange: core-shell nanocomposites with double-loaded nanoparticles (comp.GcsR) * indicates a statistically significant difference ($P < 0.05$). (For interpretation of the references to color in this figure legend, the reader is referred to the web version of this article.)

was needed for the same inhibitory effect (0.093 $mg{\cdot}mL^{-1}$). The MIC for the gentamicin antibiotic alone was 3.03 $\mu g{\cdot}mL^{-1}$ which correlates well with the amount of this antibiotic found in 0.51 $mg{\cdot}mL^{-1}$ of GCS nanoparticles (2.96 $\mu g{\cdot}mL^{-1}$). However it indicates that the maximum concentration of gentamicin released by GCSR at their inhibitory dose, 0.55 $\mu g{\cdot}mL^{-1}$, is below the antibiotic MIC. On the contrary, at this GCSR particle dose, the rifamycin concentration is 0.062 $\mu g{\cdot}mL^{-1}$, thus larger than the MIC of this antibiotic (0.055 $\mu g{\cdot}mL^{-1}$). This suggests that the inhibitory effect of double-loaded particles is mainly due to the presence of rifamycin. Furthermore, the synergistic effect of the rifamycin-gentamicin combination on *S. aureus* was assayed and no synergistic activity was observed by the checkerboard method [22]. However, these results stand only for *S. aureus*, that is much more sensitive to rifamycin than to gentamicin, as indicated by that the two orders of magnitude difference in their MICs, while different results could be expected for other bacteria, such as *P. aeruginosa*, that is much more sensitive to gentamicin than to rifamycin.

In a second step, nanocomposites were obtained by mixing acidic solution of type I collagen extracted and purified from rat tail tendon (5 $mg{\cdot}mL^{-1}$) with silica nanoparticles at a 0.5 M (30 $mg{\cdot}mL^{-1}$) final concentration. SEM imaging evidences that the fibrillar collagen organization with its typical periodic banding pattern was not significantly altered by the addition of double-loaded core-shell nanoparticles that were highly entangled in the protein network (Fig. 2).

The antibiotic-release properties of the resulting hydrogels were first evaluated *in vitro* by the disk diffusion method according to the United States Pharmacopeia using a *S. aureus* suspension. The antibacterial efficiency was evaluated from the diameter of the resulting bacteria-free area (inhibition zone) around the nanocomposite that was compared to a calibration curve established from antibiotic-impregnated paper disks [8]. Nanocomposites incorporating double-loaded nanoparticles showed a sustained antibacterial activity over the 10 day-period of investigation (Fig. 3). Composites with a gentamicin-loaded core but an unloaded shell also showed a preserved activity over this period. However, from day 2, they exhibited a smaller antibacterial efficiency than the double-loaded systems, reaching 50% of their activity after 10 days. Considering the particle concentration within the hydrogel (30 $mg{\cdot}mL^{-1}$), the maximum gentamicin concentration that can be released is *ca.* 120 $\mu g{\cdot}mL^{-1}$, well above the MIC of this antibiotic. As a matter of fact, the relative antimicrobial activity for the GCS particles within the hydrogel is *ca.* 150% compared to a 60 $\mu g{\cdot}mL^{-1}$ gentamicin reference after 1 day, suggesting that a large fraction of this antibiotic is rapidly released. In the case of the double-loaded particles, rifamycin is present at the outer surface and should be released first while gentamicin may contribute to the higher maintained activity on the longer term. This assumption is supported by previous data showing the dual release of the two antibiotics from these particles when tested against *S. aureus* and *P. aeruginosa* [14]. However, whereas rifamycin and gentamicin were completely released from the particles in suspension within 3 h and 20 h [14], respectively, their encapsulation within the collagen hydrogel extends the release time up to 10 days. To explain such an extension, it must be reminded that the release from silica nanoparticles is due to the solubility of silica in water. In neutral buffer at 37 °C and for non-porous particles, the process of dissolution occurs by surface erosion, leading to the release of the encapsulated drugs. As shown on the SEM images here, in the nanocomposites, the silica particles are surrounded by collagen fibers. Such a coating can decrease the accessibility of the particle surface to the water and therefore slow down the erosion process and the release rate.

With the aim of evaluating the biocompatibility of nanocomposites, an acute irritation test was performed in albino rabbits following the OECD Guidelines for the testing of chemicals. After the nanocomposite removal, the signs of erythema and edema were observed over a 72 h period. As illustrated in Fig. 4, the skin of tested albino rabbits showed no signs of edema or erythema over this period, thereby evidencing the good tolerance of healthy skin for the nanocomposites. These results add up to the previous demonstration that collagen-bare silica nanocomposites do not trigger severe immune response when implanted in subcutaneous pockets [23].

In order to evaluate the performance of nanocomposites to combat or prevent infection in cutaneous wounds, the materials were administered *in vivo* in a model of infected wound. The capability of antibiotics-loaded nanocomposites to reduce the number of bacteria in infected skin was measured. After infection with a *Staphylococcus aureus* suspension, 200 µL double-loaded or unloaded nanocomposites (control) were applied to the injured skin. After a 48 h period, a reduction of more than two orders of magnitude of CFU per cm^2 of skin was

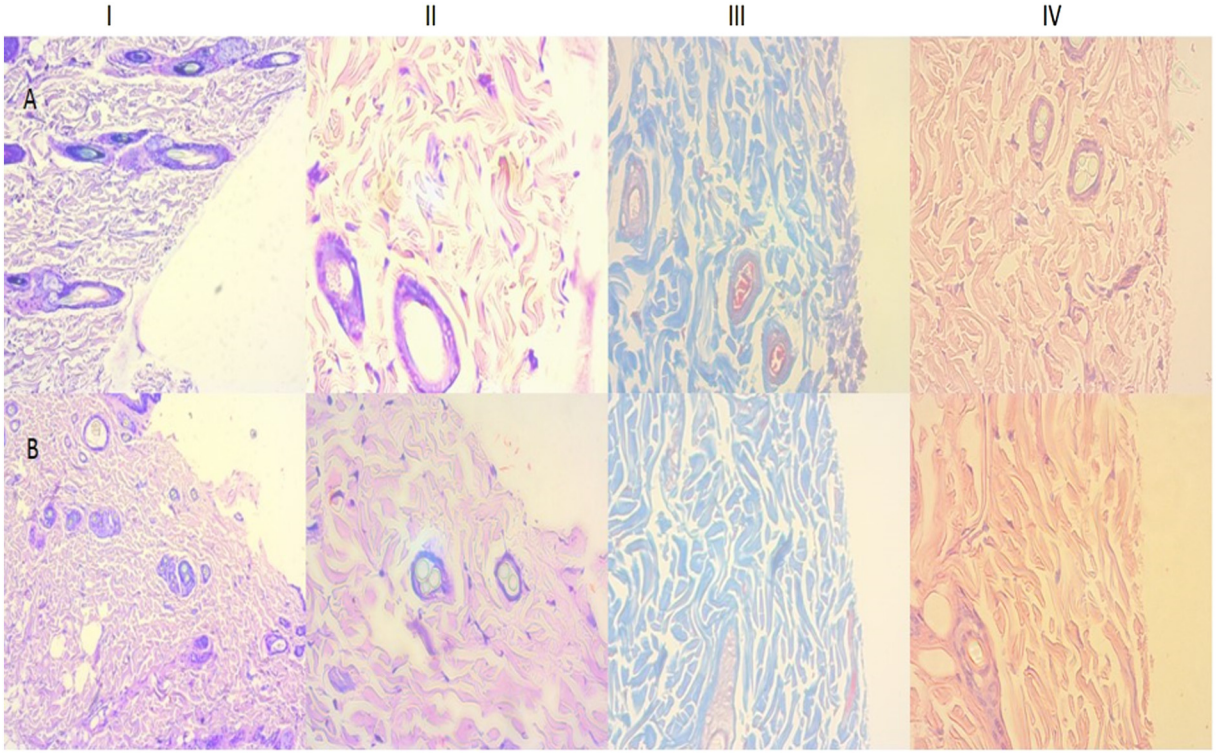

Fig. 6. Rat skin treated with unloaded (A) or double loaded (B) nanocomposites. I: 10× Giemsa, II: 40× Giemsa, III: 40× Masson's trichrome, IV: 40× Hematoxylin-Eosin staining.

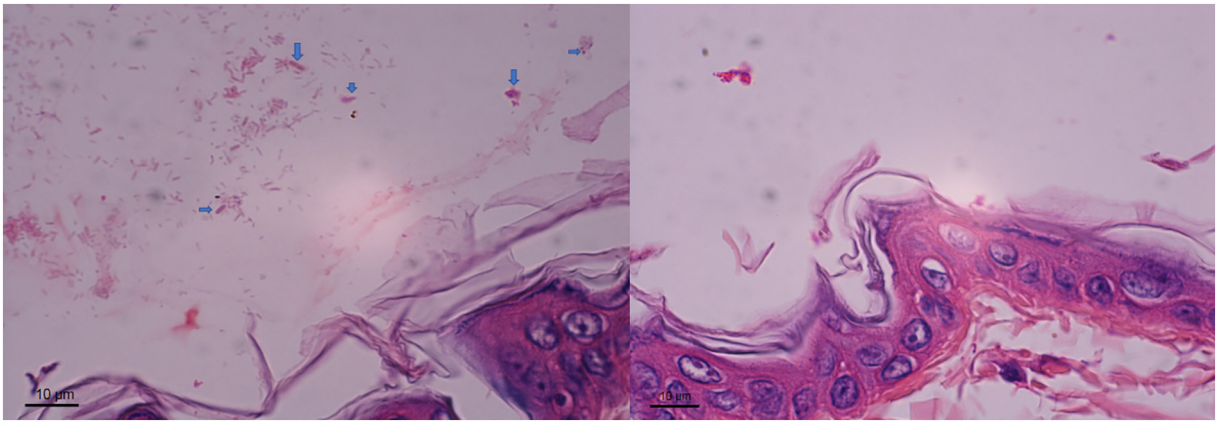

Fig. 7. Giemsa staining at 100× of rat skin treated with unloaded core-shell (left) or with GCSR nanocomposites after *S. aureus* inoculation, showing inoculated bacteria (blue arrow). (For interpretation of the references to color in this figure legend, the reader is referred to the web version of this article.)

observed when the nanocomposites were double-loaded with gentamicin and rifamycin (4.51 ± 0.04 logs for loaded particles *versus* 6.75 ± 0.70 logs for unloaded ones ($P < 0.05$)) (Fig. 5). Compared to the $5 \cdot 10^5$ bacteria initially introduced, the amount of remaining *S. aureus* after contact with the loaded nanocomposites is *ca.* $3 \cdot 10^4$ while it is *ca.* $5 \cdot 10^6$ with the unloaded ones.

To evaluate the resolution of inflammation by nanocomposites, Giemsa staining and immunodetection of macrophages were performed on infected dermis. The dermal tissue located below the infected wound was embedded in paraffin and histological sections were carried out. First, a Giemsa staining was performed to observe the presence of immune cells within dermis. Histological examination of uncontaminated wound (control) did not show any clear evidence of adverse reaction after exposure to double loaded core-shell nanocomposites, supporting the biocompatibility of the developed materials. In contrast, the presence of inoculated bacteria (blue arrow) as well as the presence of a bacilli natural contamination in tissues treated with unloaded nanocomposites (no antibiotics) confirmed the suitability of the superficial infection model [19], meanwhile the small number of visible bacteria in skin treated with double-loaded nanocomposites evidenced the efficiency of these materials in controlling superficial skin infections (Figs. 6 and 7). In a second step, the immunodetection of macrophages using the CD-68 antibody was carried out as described elsewhere [24]. Macrophages are key cells in the process of wound healing because they allow the transition between the inflammatory phase and the proliferative phase. After an injury, inflammation occurs. After 2 days, a large number of inflammatory macrophages (phenotype M1) expressing the CD-68 marker are observed [25]. Under the effect of cytokines such as IL-4, IL -13 or IL-10, the M1 phenotype turns to a wound healing M2 phenotype. In chronic wounds, macrophages are stuck in the M1 phenotype, which is favored by the bacterial infection. Hence resolving infection tends to solve chronic inflammation. As expected M1

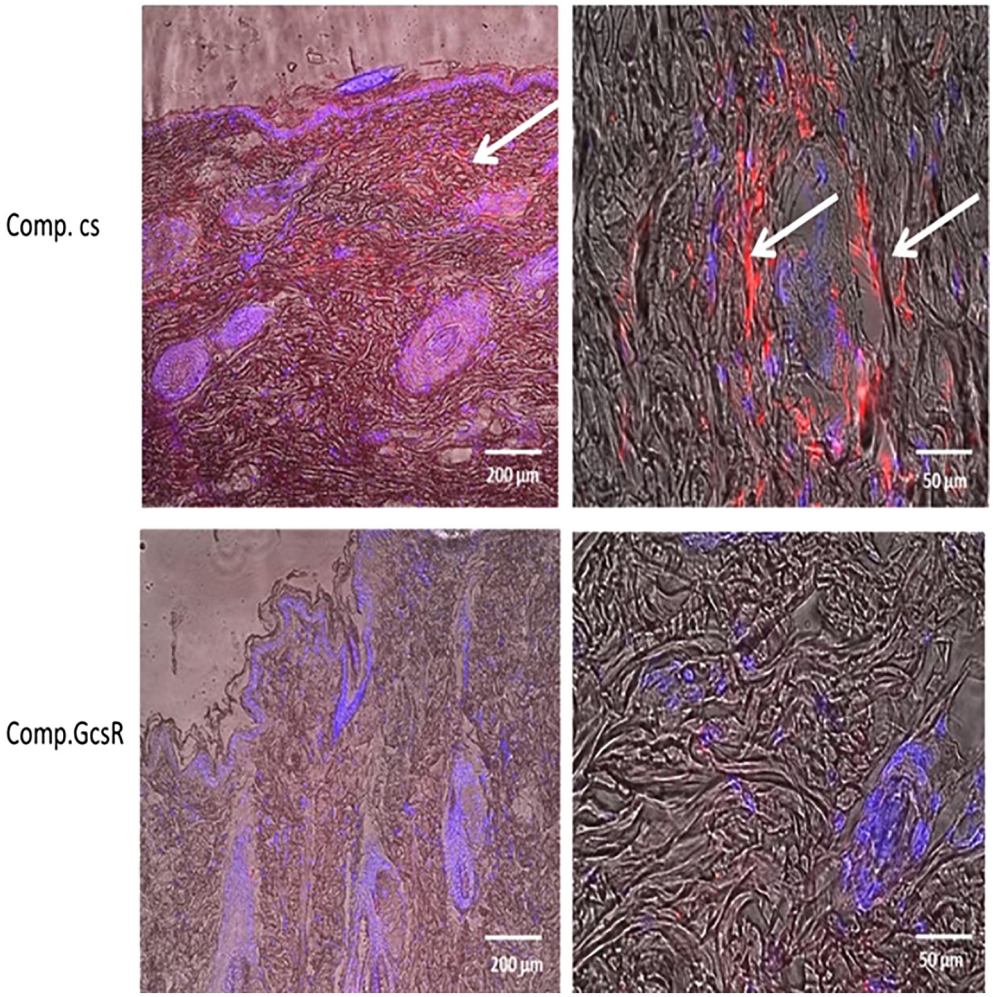

Fig. 8. Immunodetection inflammatory macrophages (phenotype M1) CD-68 (white arrows, red staining) in animal treated with unloaded (comp.cs) and double-loaded (comp.GcsR) composites. Cells nuclei are stained in blue by DAPI. (For interpretation of the references to color in this figure legend, the reader is referred to the web version of this article.)

macrophages were here observed in the top part of infected dermis when unloaded nanocomposites were applied to the wound (Fig. 8). In contrast, no CD-68-stained macrophages were visible when antibiotics-loaded materials were applied, evidencing the performance of loaded nanocomposites to solve infection-triggered inflammation.

4. Conclusions

Taken together, these results show the effectiveness of drug-loaded collagen-silica nanocomposites to combat infection. These nanocomposites allow the sustained and topical release of two antibiotics within the wound bed, decrease the number of bacteria inside the wound by 2 log steps and solve the associated inflammation. In addition, they are well-tolerated by skin, supporting their potentiality in clinical applications. The local topical release of antibiotics such as gentamicin and rifamycin is an advantage compared to the systemic administration because it limits possible side effects. In addition, the possibility to deliver different antibiotics with a large spectrum at the same time may provide a suitable response to bacterial multi-resistance.

Acknowledgements

The authors would like to acknowledge the support of grants from the Universidad de Buenos Aires UBACYT 20020150100056BA, from CONICET PIP 11220120100657CO, from Agencia Nacional de Investigaciones Cientificas y Técnicas PICT 2015-2922 and from the PICS program of CNRS. This work has the approval of the ethical committee of Facultad de Farmacia y Bioquímica, Universidad de Buenos Aires.

References

[1] S. Das, A.B. Baker, Biomaterials and nanotherapeutics for enhancing skin wound healing, Front. Bioeng. Biotechnol. 4 (2016), https://doi.org/10.3389/fbioe.2016.00082.
[2] C. Dhand, M. Venkatesh, V.A. Barathi, S. Harini, S. Bairagi, E. Goh Tze Leng, N. Muruganandham, K.Z.W. Low, M.H.U.T. Fazil, X.J. Loh, D.K. Srinivasan, S.P. Liu, R.W. Beuerman, N.K. Verma, S. Ramakrishna, R. Lakshminarayanan, Bio-inspired crosslinking and matrix-drug interactions for advanced wound dressings with long-term antimicrobial activity, Biomaterials 138 (2017) 153–168, https://doi.org/10.1016/j.biomaterials.2017.05.043.
[3] M.I. Alvarez Echazú, C.E. Olivetti, C. Anesini, C.J. Perez, G.S. Alvarez, M.F. Desimone, Development and evaluation of thymol-chitosan hydrogels with antimicrobial-antioxidant activity for oral local delivery, Mater. Sci. Eng. C 81 (2017) 588–596, https://doi.org/10.1016/j.msec.2017.08.059.
[4] C. Helary, M.F. Desimone, Recent advances in biomaterials for tissue engineering and controlled drug delivery, Curr. Pharm. Biotechnol. 16 (2015) 635–645.
[5] R.G. Gourdie, T.A. Myers, A. McFadden, Y. Li, J.D. Potts, Self-organizing tissue-engineered constructs in collagen hydrogels, Microsc. Microanal. 18 (2012) 99–106, https://doi.org/10.1017/S1431927611012372.
[6] W. Friess, Collagen – biomaterial for drug delivery1dedicated to Professor Dr. Eberhard Nürnberg, Friedrich-Alexander-Universität Erlangen-Nürnberg, on the occasion of his 70th birthday.1, Eur. J. Pharm. Biopharm. 45 (1998) 113–136, https://doi.org/10.1016/S0939-6411(98)00017-4.
[7] Y. Lan, W. Li, Y. Jiao, R. Guo, Y. Zhang, W. Xue, Y. Zhang, Therapeutic efficacy of antibiotic-loaded gelatin microsphere/silk fibroin scaffolds in infected full-thickness

burns, Acta Biomater. 10 (2014) 3167–3176, https://doi.org/10.1016/j.actbio.2014.03.029.
[8] G.S. Alvarez, C. Helary, A.M. Mebert, X. Wang, T. Coradin, M.F. Desimone, Antibiotic-loaded silica nanoparticle-collagen composite hydrogels with prolonged antimicrobial activity for wound infection prevention, J. Mater. Chem. B 2 (2014) 4660–4670, https://doi.org/10.1039/C4TB00327F.
[9] L. Jiang, C.R.R. Gan, J. Gao, X.J. Loh, A perspective on the trends and challenges facing porphyrin-based anti-microbial materials, Small 12 (2016) 3609–3644, https://doi.org/10.1002/smll.201600327.
[10] C. Bebbington, G. Yarranton, Antibodies for the treatment of bacterial infections: current experience and future prospects, Curr. Opin. Biotechnol. 19 (2008) 613–619, https://doi.org/10.1016/j.copbio.2008.10.002.
[11] G. Tiwari, R. Tiwari, S. Bannerjee, L. Bhati, S. Pandey, P. Pandey, B. Sriwastawa, Drug delivery systems: an updated review, Int. J. Pharm. Investig. 2 (2012) 2, https://doi.org/10.4103/2230-973X.96920.
[12] T. Bollenbach, Antimicrobial interactions: mechanisms and implications for drug discovery and resistance evolution, Curr. Opin. Microbiol. 27 (2015) 1–9, https://doi.org/10.1016/j.mib.2015.05.008.
[13] R. Lakshminarayanan, R. Sridhar, X.J. Loh, M. Nandhakumar, V.A. Barathi, M. Kalaipriya, J.L. Kwan, S.P. Liu, R.W. Beuerman, S. Ramakrishna, Interaction of gelatin with polyenes modulates antifungal activity and biocompatibility of electrospun fiber mats, Int. J. Nanomedicine 2439 (2014), https://doi.org/10.2147/IJN.S58487.
[14] A.M. Mebert, C. Aime, G.S. Alvarez, Y. Shi, S.A. Flor, S.E. Lucangioli, M.F. Desimone, T. Coradin, Silica core-shell particles for the dual delivery of gentamicin and rifamycin antibiotics, J. Mater. Chem. B 4 (2016) 3135–3144, https://doi.org/10.1039/C6TB00281A.
[15] J. Wu, Y. Zheng, X. Wen, Q. Lin, X. Chen, Z. Wu, Silver nanoparticle/bacterial cellulose gel membranes for antibacterial wound dressing: investigation *in vitro* and *in vivo*, Biomed. Mater. 9 (2014) 035005, , https://doi.org/10.1088/1748-6041/9/3/035005.
[16] L.C.J. Thomassen, A. Aerts, V. Rabolli, D. Lison, L. Gonzalez, M. Kirsch-Volders, D. Napierska, P.H. Hoet, C.E.A. Kirschhock, J.A. Martens, Synthesis and characterization of stable monodisperse silica nanoparticle sols for *in vitro* cytotoxicity testing, Langmuir 26 (2010) 328–335, https://doi.org/10.1021/la902050k.
[17] J. Wu, J. Silvent, T. Coradin, C. Aimé, Biochemical investigation of the formation of three-dimensional networks from DNA-grafted large silica particles, Langmuir 28 (2012) 2156–2165, https://doi.org/10.1021/la2037372.
[18] N. Rajan, J. Habermehl, M.-F. Cote, C.J. Doillon, D. Mantovani, Preparation of ready-to-use, storable and reconstituted type I collagen from rat tail tendon for tissue engineering applications, Nat. Protoc. 1 (2007) 2753–2758, https://doi.org/10.1038/nprot.2006.430.
[19] E. Kugelberg, T. Norström, T.K. Petersen, T. Duvold, D.I. Andersson, D. Hughes, Establishment of a superficial skin infection model in mice by using *Staphylococcus aureus* and *Streptococcus pyogenes*, Antimicrob. Agents Chemother. 49 (2005) 3435–3441.
[20] OECD, Test No. 404: Acute Dermal Irritation/Corrosion, Organ. Econ. Co-Oper. Dev, 2002, https://doi.org/10.1787/9789264070622-en.
[21] J.M. Andrews, Determination of minimum inhibitory concentrations, J. Antimicrob. Chemother. 48 (Suppl. 1) (2001) 5–16.
[22] G. Orhan, A. Bayram, Y. Zer, I. Balci, Synergy tests by E test and checkerboard methods of antimicrobial combinations against *Brucella melitensis*, J. Clin. Microbiol. 43 (2005) 140–143, https://doi.org/10.1128/JCM.43.1.140-143.2005.
[23] M.F. Desimone, C. Hélary, S. Quignard, I.B. Rietveld, I. Bataille, G.J. Copello, G. Mosser, M.-M. Giraud-Guille, J. Livage, A. Meddahi-Pellé, T. Coradin, *In vitro* studies and preliminary *in vivo* evaluation of silicified concentrated collagen hydrogels, ACS Appl. Mater. Interfaces 3 (2011) 3831–3838, https://doi.org/10.1021/am2009844.
[24] C. Helary, A. Abed, G. Mosser, L. Louedec, A. Meddahi-Pellé, M.M. Giraud-Guille, Synthesis and *in vivo* integration of improved concentrated collagen hydrogels, J. Tissue Eng. Regen. Med. 5 (2011) 248–252, https://doi.org/10.1002/term.326.
[25] T. Lucas, A. Waisman, R. Ranjan, J. Roes, T. Krieg, W. Muller, A. Roers, S.A. Eming, Differential roles of macrophages in diverse phases of skin repair, J. Immunol. 184 (2010) 3964–3977, https://doi.org/10.4049/jimmunol.0903356.